This paper can be found at https://doi.org/10.1061/(ASCE)ST.1943-541X.0002437

Nonlinear Dynamic Analysis for Safety Assessment of Heritage Buildings: Church of Santa Maria de Belém

João Roque[1], Daniel V. Oliveira[2], Tiago Miguel Ferreira[3], Paulo B. Lourenço[4]

[1] *Adjunct Professor, Department of Applied Mechanics, Polytechnic Institute of Bragança, Portugal - jroque@ipb.pt*

[2] *Associate Professor, ISISE, Institute of Science and Innovation for Bio-Sustainability (IB-S), Department of Civil Engineering, University of Minho, Portugal - danvco@civil.uminho.pt*

[3] *Postdoc Researcher, ISISE, Institute of Science and Innovation for Bio-Sustainability (IB-S), Department of Civil Engineering, University of Minho, Portugal - tmferreira@civil.uminho.pt (corresponding author)*

[4] *Full Professor, ISISE, Institute of Science and Innovation for Bio-Sustainability (IB-S), Department of Civil Engineering, University of Minho, Portugal - pbl@civil.uminho.pt*

Abstract

Despite the remarkable longevity of heritage constructions, they typically present several structural fragilities inherent to their own material and constructive features. This fact is particularly relevant when seismic loads are concerned since a very significant part of such constructions lack adequate seismic resistance, requiring therefore retrofitting interventions in order to mitigate their vulnerability. However, to guarantee the success of the interventions, they should be carefully selected based on the full understanding of the dynamic response of the building and, in particular, of its most vulnerable structural elements. Due to many reasons, the issues associated with this kind of analysis are still difficult to address and therefore research on this subject should be encouraged. Taking this into account, the church of *Santa Maria de Belém*, one of the most

emblematic buildings of the Monastery of *Jerónimos* complex, in Lisbon, is used in this work as a case study to discuss the non-linear dynamic response of cultural heritage buildings. The non-linear dynamic behaviour of the church is numerically simulated with a 3D model using artificially generated seismic acceleration time histories, in agreement with seismic hazard scenarios for return periods of 475, 975 and 5000 years. The dynamic response of the church is discussed and a comparison against results derived from a pushover analysis is also performed. Finally, a modal analysis is performed to estimate the damage level present in the church after the occurrence of such seismic scenarios.

Introduction

Earthquakes continue to represent a serious threat all over the world, in particular for Mediterranean countries wherein these events have been triggering significant destruction and loss over the last decades. Despite the unpredictable nature of earthquakes, seismic risk assessment should be addressed having in mind the main cause of damage, which is related to inadequate seismic resistance of the existing structures, either residential, industrial or cultural heritage buildings (Maio and Tsionis 2016). Like in many other European countries, a large part of the Portuguese cultural heritage is made of unreinforced masonry buildings. Despite their remarkable longevity, such buildings lack of adequate seismic resistance, calling into question not only their preservation, but also the safety of people and goods. In order to change this reality, it is necessary to support the development of new knowledge on this specific field and form the basis for the establishment of more efficient protection measures towards the safeguard of this valuable heritage (Ferreira et al. 2015b).

The analysis of the structural response of ancient masonry buildings in general (D'Ayala 2013; Lagomarsino and Resemini 2009), and of monumental buildings in particular (Betti and Vignoli 2011; Milani and Valente 2015a), is a very challenging task. Its geometry is frequently complex, and the properties and the internal structure of their constituting materials are often extremely

difficult to define, which necessarily limits the selection of the approach to be applied (Lourenço 2002; Valente and Milani 2016). Actually, none of the currently applied static analysis techniques (Araujo et al. 2012; Gattulli et al. 2013; Milani 2013; Milani and Venturini 2011; 2013) can be successfully used to assess the seismic safety of monumental buildings.

To help practitioners, the Italian Guidelines for the Cultural Heritage (DPCM 2011) suggest the use of a quite rough approach as to obtain the acceleration at collapse. It is based on the pre-assignment of partial failure mechanisms and on the utilization of the kinematic theorem of limit analysis within the assumption of a no-tension material model for masonry. However, such approach presents some evident drawbacks, as for instance the risk of overestimating the horizontal acceleration at failure due to the incorrect identification of failure mechanisms and the geometrical simplifications introduced in the model. Non-linear static analysis, also known as pushover analysis, represents a current alternative to limit analysis (Betti et al. 2015; Milani and Valente 2015b). However, as well known, non-linear static analysis conducted when the global behaviour beyond the maximum load carrying capacity is required cannot be easily obtained using refined finite element modelling with many 2D and 3D elements, as needed for a realistic analysis of masonry churches (Milani and Valente 2015b). Moreover, complex material models are not usually implemented in most of the commercial codes available for standard design. From this, it seems clear that, despite the level of complexity of the finite element analysis, which makes them almost unusable for most practitioners, the limits of applicability of non-linear static approaches should be handled with great care.

In this context, this paper aims to contribute to the discussion on the non-linear dynamic analysis of monumental buildings, by using the church of *Santa Maria de Belém* (also known as the Church of the Monastery of *Jerónimos*) as a case study. Integrated within the Monastery of *Jerónimos* complex, this UNESCO World Heritage monument is considered one of the most extraordinary examples of Portuguese architectural heritage. The non-linear dynamic response of the church is analysed herein with a 3D model built in DIANA® software (TNO Building and

Construction 2016) and the results, obtained from artificially generated far-field earthquake records associated with medium to high seismic risk scenarios in Portugal (Carvalho et al. 2009) for increasing return periods (475, 975 and 5000 years) are comprehensively discussed. The analysis is focused on the critical elements of the structure previously identified (Masciotta et al. 2016), and complimentary by the performed pushover analysis, whose performance is assessed on the basis of several structural outputs, namely bending moment-curvature diagrams and stress-strain curves. In addition, the global response of the church is evaluated in terms of base shear, including the outcomes from the pushover analysis, and finally, a post-action modal analysis is carried out to estimate the level of modal damage present in the church.

It is important to stress that, although the structural behaviour of the church of *Santa Maria de Belém* has already been addressed in some past research works, namely in (Lourenço et al. 2007; Ramos et al. 2010; Masciotta et al. 2016), none of those have been focused on the non-linear dynamic response of the monument, and therefore this paper represents an important contribution towards the understanding of its seismic behaviour. In addition, taking into account that very few time history analysis have been used to date to assess the seismic performance of monumental constructions (which still remains a true challenge), it is also intended that this work may serve as a representative example of how similar issues in analogue heritage structures can be addressed.

The church of Santa Maria de Belém

Built during the 16th century (started in January 1501 and finished about 100 years later), the church of *Santa Maria de Belém* belongs to the Monastery of Jerónimos complex, one of the most notable examples of Late Gothic Manuelino style of Portuguese architecture (see Figure 1). The church and the monastery symbolise the Portuguese age of discovery and are among the most

important and visited tourist attractions of Lisbon. In 1983, it was formally nominated by UNESCO as a World Heritage Site.

The monastery stretches over an area of approximately 300 per 50 m^2 and develops around two courts, see Figure 2 (a). The larger court is bordered by a two-storey arcade, wherein the National Archaeology Museum, the Maritime Museum, and the Central Library are hosted. The smaller court, the cloister, is bordered by the sacristy, the chapter room, the refectory and the church of *Santa Maria de Belém*, object of this research. In geometrical terms, the church is 70 m long, 23 m wide (40 m in the transept), and 24 m high. As can be observed in Figure 2 (b), geometrically the church presents a cruciform layout with a single nave crossed by a transept with two lateral chapels and a chancel. The roof is composed of a single rib-vaulted ceiling of 30 m span, see Figure 2 (c), supported by six columns with circular base. A single bell tower of 50 m height rises from the corner between south and west façades.

The church is made of large blocks of a white fossiliferous limestone, called "*calcário de lioz"*, which were quarried close by. The naves are covered with a slightly curved barred vault provided with stone ribs according to a spider web pattern. Two rows of octagonal columns, with a free height of 16 m and a radius ranging from 1.04 m (in the nave columns) to 1.88 m (in the nave-transept columns), divide almost imperceptibly the longitudinal naves, creating almost a single nave. The columns are connected to the vault by means of large fan capitals that reduce the free span of the nave.

The thickness of the walls varies from side to side, ranging from 1.90 m in the south wall to 2.65 m in the east walls (chancel side). Due to the presence of an internal staircase that provides access to the choir, the cloister and the bell tower, the north wall presents about 3.5 m thickness. The south wall is cut by large openings and its stability is ensured by three trapezoidal buttresses, which are not aligned with the columns, indicating that the south wall is prior to the construction of the vault. On the top of the vaults, brick masonry wallets, built during the 1930's, provide support for the roofing tiles.

This paper can be found at https://doi.org/10.1061/(ASCE)ST.1943-541X.0002437

Description and calibration of the numerical model

The numerical model of the church was prepared using the Finite Element (FE) software DIANA® (TNO Building and Construction 2016). As discussed in detail within the following sections, given the size and the great complexity of the structure, it was necessary to adopt geometrical simplifications in the FE model to allow for an extensive non-linear dynamic analysis, within acceptable processing time. However, special attention was given into the discretization of the model in order to reproduce the geometrical stiffness of the church as close to reality as possible. The geometry of the 3D model and the mechanical properties of the materials, discussed in Sections 3.1 and 3.2, respectively, were defined herein based on a set of non-destructive and laboratory tests (Roque 2010; Masciotta et al. 2016).

Geometry

The full numerical model is composed of 2684 Timoshenko beam elements with quadratic interpolation and 4242 nodes, corresponding to a total of 25452 degrees of freedom (DoF), see Figure 3. The supports were fully restrained, being rotations possible given the non-linear material behaviour assumed.

Special attention was paid to the modelling of the vault and the piers of the nave, Figure 4 (a) and (b). As detailed in Figure 4 (c) and (d), the ribs profiles of the vault were modelled by beam elements with trapezoidal cross section, whereas a T shaped cross-section was adopted for the rib-slab system. Given its marginal contribution to the structural response, the mortar layer covering the stone slabs was considered only in terms of equivalent mass.

Regarding the columns, depicted in Figure 5, the octagonal geometry of the shaft was approximated by beam elements having a circular cross-section. The capitals were represented at the base by elements with a cone-frustum geometry and, in the transition part to the vault, by cuneiform elements radially set out. Given the poor mechanical properties of the infill material of

the capitals, their contribution to the structural response of the church was neglected in the model. As far as the walls are concerned, they were modelled by a grid of vertical and horizontal beam elements. It is worth noting that their mass was assigned to the vertical elements in order to avoid the occurrence of marginal flexural stresses due to gravity load in the horizontal elements.

Material properties and model parameters

A wide range of sophisticated mechanical models have been developed over the past years to predict the non-linear behaviour of masonry material both in tension (low tensile capacity with consequent cracking phenomena) and compression, including individual failures and damage mechanisms (Ferreira et al. 2015a). Unfortunately, some of these models are rather difficult to apply to the 3D analysis of complex structural systems, not only due to the large number of parameters involved in the definition and updating of the mechanical model, but also because of the amount of DoF required to mesh the structure (Betti et al. 2011).

Following a critical review of the non-linear material models available in the literature (Lourenço 2002), the physical non-linear behaviour of the masonry material was simulated in this work using a distributed plasticity formulation based on the Total Strain Crack Model, detailed in (TNO Building and Construction 2016). A parabolic stress-strain relation was used, where the compressive strength, f_c, was assumed equal to 10 MPa (estimated from a reference value obtained experimentally by taking into account the dispersion of the results, CV≈30%, and a safety factor for ancient masonry equal to 3.0; further details on this can be found in (Roque 2010; Masciotta et al. 2016)) and a tensile strength, f_t, equal to 0.01 MPa. The fracture energy in compression, G_C, is equal to 16 kJ/m^2. The post-cracking shear behaviour was modelled assuming a constant value for the shear retention faction, β, equal to 0.01 (Scotta et al. 2001), which means no post-peak shear capacity. Finally, the material was assumed to be

homogeneous, with an elastic modulus, *E*, calibrated with in-situ tests and 0.2 for the Poisson's ratio, υ. The weight per volume unit, γ, adopted for the masonry material was 24 kN/m^3.

Calibration procedure

Once built, the numerical model described in the previous sections was calibrated, both in the linear and nonlinear domains, from a set of experimental and numerical results. In the first phase (linear domain), the results of the static linear analyses were compared with corresponding results obtained from a partial numerical model of the nave, wherein 3D elements were used to study the behaviour of the vault under vertical actions (Lourenço et al. 2007). Following this procedure, it was possible to calibrate the geometric stiffness of some the church substructures, namely the vault curvatures. In a second phase, based on the experimental results obtained from the dynamic identification of the columns and the nave vault (further details on this work can be found in (Roque 2010; Masciotta et al. 2016)), and from the mechanical characterisation of the masonry, the elastic modulus of the columns and the equivalent stiffness of the remaining substructures of the church were assumed to be equal to 30 GPa and 12 GPa, respectively. The first 16 numerical mode shapes found for the church are essentially related with resonant frequencies of the main nave and their columns. Table 1 presents the best correlations found between the experimental and the calibrated numerical eigenfrequencies for nave and columns, including the corresponding error.

With the intend to perform nonlinear dynamic analyses, as the adjacent buildings provide restraint effects on the church, a part of them was included in the geometrical model with a coarse mesh to limit the computational-effort. Sensitive modal analyses were performed until the results were independent of the included volume. Also the parabolic stress-strain relation adopted to perform nonlinear dynamic analyses was adjusted based on some previous sensitive pushover

analysis as their results were showing an unfeasible available ductility in compression, for masonry material, when a preliminary perfect elastic-plastic material relation was used.

After the above referred calibration procedures, the results collected by the long-term static monitoring system, revealing the presence of cyclic oscillations on the top of the nave columns due to seasonal fluctuations of the temperature (with a rate of about 0.01mm/m/ºC, see Roque 2010; Masciotta et al. 2016), were used to check the ability of the model to reproduce them. Also, the accelerations due to a low seismic event (occurred in February 12, 2007) registered by the dynamic monitoring system were used as excitation to try to reproduce numerically the observed behavior. As post-action, very low modal frequencies changes were detected on the main nave. Considering the complexity of the structure and the model, a satisfactory numerical agreement was reproduced on both situations. Even so, in future works, it would be desirable to validate the global model resorting to refined models focused on particular structural elements (e.g. columns of the nave).

Non-linear dynamic analysis

As referred above, the seismic response of the church of *Santa Maria de Belém* was evaluated resorting to linear static, non-linear static and non-linear dynamic approaches. Although this paper is focused on the non-linear dynamic analysis of the structure, the results obtained from linear and non-linear static analyses, presented in (Masciotta et al. 2016), are fundamental to better understand the non-linear dynamic response of the structure and therefore the most important remarks obtained from those analyses are synthetized next: the bearing capacity of the church under gravity loading is considerably affected by the structural behaviour of the nave columns behaviour; the collapse mechanism of the church under gravity loads is associated with the failure of the north column of the central arcade, which presents a sudden loss of bearing capacity related

to the increase of the horizontal and vertical displacements; and despite the high slenderness of the columns, the structural performance of the church for vertical loading is good.

The non-linear dynamic analysis performed in this work aimed at investigating the seismic behaviour of the church, paying particular attention to the early identified vulnerabilities. To achieve that, a series of acceleration time histories were initially selected taking into consideration the two principal seismological areas susceptible to affect the city of Lisbon: the first located in the adjacent Atlantic zone, in the southeast of São Vicente cape (far-field scenario); and the second one located in the north of Lisbon, at Lower Tagus Valley (near-field scenario).

Due to the lack of consistent real seismic records in mainland Portugal, authors have resorted to artificial records generated by the Earthquake Engineering and Structural Dynamics Division department (NESDE) at the National Laboratory of Civil Engineering (LNEC), Lisbon, which main features can be found in (Carvalho et al. 2004). Based on scenarios presented by (Sousa 2006), acceleration time series were synthetized for each return period, considering only the Atlantic seismic source, which corresponds to a far-field earthquake. In addition, given the importance of the building, scenarios with return periods of 5000 years were also considered. Ten accelerograms were generated for each return period. Of those, due to the long time required to carry out the non-linear dynamic analyses, only the three characterised in Table 2 were actually used. For all generated accelerograms, the focal distance was equal to 205 km and the frequency content was similar, the selection of those three signals was based on their sustained maximum acceleration (SMA). For an easy interpretation, each analysis is named with an acronym (input ID in Table 2), where the prefix indicates the return period (475, 975 or 5000), the central text refers to the magnitude (7.4, 7.8 or 8.2) and the final part is associated to the analysis number (1 to 3). The acronym PGA in the table is the peak ground acceleration.

All numerical simulations were performed with DIANA® software (TNO Building and Construction 2016) considering material and geometric non-linear behaviour and using the

regular Newton-Raphson method combined with an energy convergence criterion established as lower or equal to 10^{-3}. The Hilber-Hughes-Taylor (HHT) method was used to integrate the system of differential equations of motion with a parameter α=-1/3 to control the numerical damping (Hilber et al. 1977). Following the established formulation for time step integration ($\Delta t<0.1T_{min}$) and considering 7.5 Hz as the highest significant frequency of interest (the dominant numerical frequencies of the nave and columns within the first 16 modes are under 7.51Hz, see Table 1), a time step Δt=0.01s was adopted.

Viscous Rayleigh damping formulation was used in order to take into account the energy dissipation mechanisms not associated with the hysteretic behavior of the structure. A low damping coefficient (ξ=1.5%) was adopted in order to avoid Rayleigh overdamping and to promote the hysteretic damping (Roque 2010). Since the central arcade, transversal to the nave, had been identified as the potentially most vulnerable sub-structure of the church, see Figure 3(c), the next discussions will be mainly focused on this part. Moreover, the behaviour of the south tower belfry is also addressed.

Seismic structural performance assessment: results and data interpretation

With the fundamental aim of identifying the occurrence of potential structural collapses for the different return periods considered (475, 975 and 5000 years), the time history response of the structure is investigated in terms of the following parameters: vertical reaction of the columns; vertical displacement of the vault key; horizontal displacement of the columns; horizontal top displacement of the north and south walls; horizontal displacement of the top node of the tower belfry and the normal tensile stress of its vertical elements. From the analysis of the results obtained for the seismic scenarios with a return period of 475 and 975 years, no indication of potential collapse of the church was found. However, for a return period of 5000 years it was possible to observe relevant changes in the structural response of the church, which are related to the development of partial collapse mechanisms.

In the transversal direction of the nave, the seismic response of the central arcade denotes a clear frame action (column-wall) resulting in high axial load variations in the columns ranging from -90% to +91% with respect to gravity load (return period of 5000 years), see Figure 7 and Figure 8. The changes in the structural performance can be clearly observed from the vertical reaction time-history response of the columns (Figure 8), when the collapse begins with a sudden reduction on the north column (about 12-13 s) and is accompanied by an increase on the south column.

Those changes are also in terms of horizontal deformability of the central arcade, mainly concentrated at the columns shaft. However, the low amplitude of the transversal displacements indicates a non-important contribution of the non-linear geometric effects to the structural performance of the vertical elements. Even for 5000 years scenario, during the pre-collapse phase of the columns, the small amplitude of the displacements seems to present a low contribution to the collapse onset. Indeed, the maximum transversal displacements obtained in the north column, for scenarios of 5000 years (during pre-collapse period), were 6.2 cm (0.52% drift) on the shaft, and 3.9 cm (0.21% drift) on the top. On the other hand, on the top of the lateral walls, the maximum transversal displacements obtained during pre-collapse period, was 4.1 cm (0.20% drift) and 2.6 cm (0.42% drift), respectively, in the south and north wall (at the level of the cloister roof).

In what regards the south tower belfry, even if it appears as one of the most vulnerable elements of the church, and despite the severity of the seismic scenarios with 5000 years return period, also the horizontal top displacements of the south tower belfry were rather small, presenting amplitudes lower than 2.5 cm. However, the analysis of the axial tensile stresses time history of all four vertical belfry elements (not presented here for sake of brevity) shows some occurrences with simultaneous tension in two of those elements, anticipating the development of a possible overturning collapse mechanism.

Finally, the potential collapse mode pattern, found for 5000 years return period scenario, is illustrated in Figure 10, where the collapse of the north columns and the consequent partial collapse of the nave vault can be clearly observed. Thus, these results not only confirm the higher vulnerability of the nave in the transversal direction (as observed in the previous static analyses), but also the vulnerability of the nave columns and their key role on the seismic behaviour of the church.

Earthquake-induced damage analysis

As the dynamic response of the church to the seismic excitation with 5000 years return period reveals the occurrence of potential collapse mechanisms involving the central arcade of the nave, the subsequent discussions will be focused at investigating damage on its structural elements (namely columns and walls). The response of the north column is presented in the form of bending moment-curvature diagrams and stress-strain curves (for the most compressed fibres), both at the bottom, middle and top sections. Moment-curvature diagrams presented in Figure 11(a) confirm the asymmetric behaviour of the column sections due to the seismic increase of the eccentric compression resulting from dead loads. A stiffness and flexural strength degradation of the sections is evident from the hysteretic behaviour associated with progressive damage, that culminates in total loss of strength at the bottom section. The stress-strain curves presented in Figure 11(b) also evidence the high damage under compression at the bottom and middle sections, as well as a significant level of cracking ($\varepsilon_{axial} >> \varepsilon_{ck}$) present in all sections. Being the axial strains lower than 0.5‰ at the top section, no damage in compression is found.

Applying the same reasoning to the south column, bending moment-curvature curves and stress-strain curves are given in Figure 12 for the same critical sections.

From the analysis of the moment-curvature curves presented in Figure 12(a), it can be observed that non-significant hysteresis justifies that sections haven't lost its total flexural strength

capacity in the south column. However, in the bottom section, the failure of the most compressed fibres appears as eminent (post-peak instability), see Figure 12 (b).

The asymmetric behavior of the nave columns, due to the asymmetry of the central arcade, is also apparent in the load interaction N-M diagram (axial load *versus* bending moment), presented in Figure 13, which reveals that the collapse of the central north column is conditioned by the combination of moderated axial compression loads (υ<0.40) with large bending moment values, resulting in high levels of eccentric compression in the section.

Complementarily, a schematic representation of the damage found in the base and middle sections of the north column is depicted in Figure 14. As can be observed, the collapse of the north column is characterised by a total failure in the base section (crushing of the effective section) and a partial failure in the shaft section (crushing of the most compressed fibres).

As for the lateral walls of the nave, the seismic damage was analysed in the critical section of the central buttresses by means of the moment-curvature and stress-strain curves presented in Figure 15. High levels of cracking on both walls, but low compressive damage, particularly noticeable in the north wall, were found.

Finally, with compressive stresses values lower than 1.0 MPa, quite low when compared with the maximum capacity, assumed as 10 MPa, no compressive damage is expected in the south tower belfry**.** However, normal tensile stresses and cracking were also noted in the all vertical elements of the belfry. Quite similar results were obtained with 5000_M82_2 input, and for this reason they will not be discussed here.

As a final note, it should be stressed that for scenarios of 475 and 975 years return periods, a generalized level of cracking and important states of stress remain in the nave sub-structures (columns, walls and vault) after seismic excitation.

This paper can be found at https://doi.org/10.1061/(ASCE)ST.1943-541X.0002437

Discussion of the base shear results

The base shear results in the transversal nave direction obtained from the dynamic analyses, considering different return periods, are presented and discussed in this section. The discussion will be held at two levels. Globally, considering the structural response the church, and partially, considering the sub-structures indicated in Figure 16: Zone A: tower + refectory + cloister (west part); Zone B: nave + cloister (central part); and Zone C: transept + chapels + apse + sacristy + cloister (east part). After that, a comparative analysis between static and dynamic base shear results is presented.

From the analysis of the in-plan base shear distribution (see Figure 17), the maximum base shear coefficients (defined as the ratio of the maximum base shear acting on the elastic structure to the total weight of the structure) in zones A and C are about 2 to 4 times greater than those obtained in zone B. These results reflect the contrast of the in-plan structural stiffness of the church, namely between zone B (the nave), less stiff, and zones A and C, much stiffer; possibly working as a bracing system to the structure as the modal analysis seems to confirm. The observable linear correlation between base shear values and seismic intensities (PGA), suggests a high average global stiffness of the church and its quite linear global behaviour, excepting the zone B (nave) that has a residual contribution to the global base shear coefficient.

It is worth noting that the smaller is the relative contribution, the greater is the return period, due to the damage suffered (see Figure 17). Finally, despite their important role in the structural integrity of the church, the contribution of the nave columns to base shear was found to be insignificant for all seismic scenarios considered.

In order to assess the potential relationship between the static global base shear coefficients (β), obtained through uniform pushover analysis as recommended in (Lourenço et al. 2011), and the envelope of the global base shear coefficient, obtained from the dynamic analyses (for 5000_M82_2 seismic input), both results are plotted together in Figure 18.

From the comparison of the outcomes obtained with both above referred strategies, it resulted that: (i) the collapse modes obtained are rather different. The pushover analyses led to the collapse of the columns, the walls and the vault, whereas only the north column has collapsed as a result of the dynamic analyses; (ii) the collapse of the north column occurs in both strategies, with a similar configuration; (iii) with pushover analyses, the collapse of the north column has a larger load factor (0.44g), while the south column collapse presents a smaller one (0.40g); (iv) the maximum dynamic global base shear coefficient (equivalent) is approximately half of the static shear coefficients (pushover); and (v) the columns had a residual contribution to the global base shear.

Thus, from (i) and (ii) it was possible to conclude that pushover analyses were able to identify only partly the seismic vulnerability of the church. Points (iii) and (iv) suggest that pushover analysis is only partly representative of the dynamic behaviour of the church, as its response seems to be highly influenced by dynamic effects not considered using pushover analysis. The lack of consideration of higher local modes of the nave columns in the structural response is pointed out as the main reason for this apparent lack of global representativeness. To better understand this phenomenon, the in-plan base shear distribution among the sub-structures A, B and C and the north column, considering both static and dynamic approaches (Figure 19), was analysed and some additional interesting conclusions can be drawn: (vi) the in-plan base shear distribution is, in percentage, identical in both strategies (about 38% in zone A; about 10% in zone B; and about 52% in zone C); (vii) the global base shear coefficient (0.23), obtained from dynamic analyses, considerably underestimates the north column base shear (2.90), resulting in large differences in terms of shear forces at the column (from 150kN due to pushover, to 989kN with the dynamic analyses); and (viii) the global base shear coefficients are not, in any of the strategies, representative of the behaviour of the nave columns, in particular of the north ones.

Thus, on the one hand, the contrast found between the values obtained for the global dynamic shear (reaching 0.23) and the dynamic shear coefficients in the north column (equal to 2.90) can

be attributed to dynamic effects on the north columns involving the contribution of local higher modes to the response. The high levels of acceleration (of about 3.0g) found in the north column shaft corroborated this interpretation, see Figure 20. On the other hand, the difference between the values of the global dynamic shear (0.23) and global static shear coefficients (0.44) can be interpreted as a result of the reduced representativeness of the pushover analysis for complex historical constructions as it is the present case study.

Complementarily, it is worth referring that (Peña et al. 2010) underlined the importance and the influence of the lateral load distribution on the results obtained from static analyses (pushover). In this sense, it is plausible that the global representativeness of the static analyses may increase with the use of triangular (or first mode proportional to global translation) pushover. However, authors do not recommend it for the usual out-of-plane failure analysis of historical constructions, see also Lourenço et al. (2011).

Based on the above outcomes, it should be underlined that pushover analysis may not be representative of the dynamic behaviour of the most critical structural elements of complex historical constructions, even though pushover can be efficient to detect their main global seismic vulnerabilities.

Post-action analysis

In the cases for which no apparent collapse was observed, the numerical simulation of the seismic performance of the church was followed by a post-action eigenvalue analysis, using the tangent stiffness of the damaged model, aimed to assess the earthquake-induced decay in natural frequencies, from the original to the damaged model. It is important to note that this type of analysis is not of interest when significant structural damage occurs. Significant damage, even when no collapse is observed, might render the stiffness matrix ill-conditioned with the results of such a modal analysis to be of no value. Figure 21 shows the frequencies of the 16 first vibration

modes of the church found for both situations, prior and after the seismic excitations per return period. Some important remarks can be pointed out from the modal frequency decays, reported in Figure 21, as follows:

(i) there is an average and nearly uniform reduction of about 1.5 Hz in the modal frequencies of the church (i.e, the first 16th numerical frequencies was reduced from 3.8-7.51 Hz to 2.8-5.3 Hz) suggesting an uniform stiffness reduction due to earthquake-induced damage (essentially cracking) on the church;

(ii) despite the different characteristics of the seismic inputs (both in duration and PGA), the reduced contrast found in the average modal frequencies of the church, may indicate that the resulting structural damage is more associated with the frequency content of the adopted accelerograms, rather than their peak ground acceleration or duration;

(iii) in relative terms, the greatest damage level occurs for the lowest severe scenarios, with 475 years.

The similarity between the frequency band of the resonant modes of the nave (columns and vault) - found to be between 3.8 and 7.5 Hz - and the dominant spectral content of the seismic signals used - between 3 and 7.5 Hz - seem to justify the special incidence of structural damage on the main nave (columns and vault) and an approximately uniform distribution for the different seismic hazard scenarios.

Finally, as the initial adopted Rayleigh damping ratio (1.5%) was associated to the 1st (3.8Hz) and 2nd (5.06Hz) global frequencies of the nave, it is expected that the Rayleigh damping ratio after the model being damaged is under 1,62% for the final range of frequencies (found to be between 2.8Hz and 5.3Hz).

Conclusions

This paper presents and discusses the main results obtained from the incremental non-linear dynamic analysis of the church of *Santa Maria de Belém* considering three different seismic hazard scenarios with increasing severity associated to of 475, 975 and 5000 years return periods. This work continues previous studies reported by Masciotta et al. (2016), regarding whom analysed the linear and non-linear static response of the church.

The results obtained for return periods of 475 and 975 years show that the church is expected to suffer extensive cracking, however, no partial or global ruin is predicted. For the 5000 years return period some potential partial collapses were identified involving the north columns of the nave. Also, the south tower belfry appears as one of the most vulnerable elements of the church, possibly involving its overturning.

Regardless of the scenarios, an asymmetric and clear frame-type behaviour, between walls and columns, was found in the transversal arcades of the nave, which led to high variations in the axial load of the columns. Even so, the level of compressive stress is moderate and therefore the potential collapse of the columns may be determined by eccentric compression.

In terms of deformability, drift values below 0.5% were observed in the central arcade for all seismic scenarios; even during the pre-collapse phase the non-linear geometric effects present a low contribution to the collapse onset.

Regarding the base shear analysis of the church**,** the comparison between static and dynamic results allows to stat that: (i) despite the major contribution of the nave columns to the structural integrity of the church, their contribution to the global base shear is only residual; static pushover analyses, although efficient to detect the main seismic vulnerabilities of the church, were not representative of the dynamic behaviour of some important sub-structures (as the nave columns).

The results of the modal analyses performed after seismic excitation revealed a residual average modal stiffness of about half of the initial modal stiffness of the church, showing also that the most part of the damage, specially concentrated in the nave, is associated with the 475 years return period scenario and mainly due to the excitation frequency content.

Overall, the base shear analysis presented in the paper provide a practical demonstration that pushover strategies should be addressed with great care when dealing with historical buildings, as possible dynamic effects involving the contribution of higher order modes can guide the dynamic response in a manner rather different from the static one.

Also, the post-action eigenvalue value analysis performed provides a practical demonstration of a useful way to assess the level of earthquake-induced damage, considering the decay of the natural frequencies prior and after seismic excitation.

Finally, this work also underlines that the numerical seismic assessment of large historical constructions is still a complex field and therefore research on this subject should be encouraged.

Acknowledgements

This work was partly financed by FEDER funds through the Operational Programme Competitiveness Factors (COMPETE) and by national funds through the Foundation for Science and Technology (FCT) within the scope of project POCI-01-0145-FEDER-007633. Authors are also grateful to three anonymous reviewers whose comments significantly improved the clarity of the paper.

References

Araujo, A. S., Lourenço, P. B., Oliveira, D. V., and Leite, J. (2012). "Seismic Assessment of St James Church by Means of Pushover Analysis – Before and After the New Zealand Earthquake." *The Open Civil Engineering Journal*, 6(1), 160–172.

Betti, M., and Vignoli, A. (2011). "Numerical assessment of the static and seismic behaviour of the basilica of Santa Maria all'Impruneta (Italy)." *Construction and Building Materials*, 25(12), 4308–4324.

Betti, M., Galano, L., and Vignoli, A. (2015). "Time-History Seismic Analysis of Masonry Buildings:

A Comparison between Two Non-Linear Modelling Approaches." *Buildings*, Multidisciplinary Digital Publishing Institute, 5(2), 597–621.

Betti, M., Orlando, M., and Vignoli, A. (2011). "Static behaviour of an Italian Medieval Castle: Damage assessment by numerical modelling." *Computers & Structures*, 89(21-22), 1956–1970.

Carvalho, A., Campos Costa, A., and Oliveira, C. S. (2004). "Modelos estocásticos com ruptura progressiva de falhas para a caracterização da acção sísmica. Aplicação ao sismo de Lisboa de 1 de Novembro de 1755." Guimarães, Portugal, 281–290.

Carvalho, A., Campos Costa, A., and Oliveira, C. S. (2009). "A Finite–Fault Modeling of the 1755 Lisbon Earthquake Sources." *The 1755 Lisbon Earthquake: Revisited*, Geotechnical, Geological, and Earthquake Engineering, Springer Netherlands, Dordrecht, 433–454.

D'Ayala, D. (2013). "Assessing the seismic vulnerability of masonry buildings." *Handbook of Seismic Risk Analysis and Management of Civil Infrastructure Systems*, Elsevier, 334–365.

DPCM. (2011). *Linee guida per la valutazione e la riduzione del rischio sismico del patrimonio culturale con riferimento alle Norme tecniche delle costruzioni di cui al decreto del Ministero delle Infrastrutture e dei trasporti del 14 gennaio; 2008 [Italian guidelines for the evaluation and the reduction of the seismic risk for the built heritage, with reference to the Italian norm of constructions]*. Italian Government.

Ferreira, T. M., Costa, A. A., and Costa, A. (2015a). "Analysis of the Out-of-Plane Seismic Behavior of Unreinforced Masonry: A Literature Review." *International Journal of Architectural Heritage*, Taylor & Francis, 9(8), 949–972.

Ferreira, T. M., Costa, A. A., Arêde, A., Gomes, A., and Costa, A. (2015b). "Experimental characterization of the out-of-plane performance of regular stone masonry walls, including test setups and axial load influence." *Bulletin of Earthquake Engineering*, Springer Netherlands, 13(9), 2667–2692.

Gattulli, V., Antonacci, E., and Vestroni, F. (2013). "Field observations and failure analysis of the Basilica S. Maria di Collemaggio after the 2009 L'Aquila earthquake." *Engineering Failure Analysis*, 34, 715–734.

Hilber, H. M., Hughes, T. J. R., and Taylor, R. L. (1977). "Improved numerical dissipation for time integration algorithms in structural dynamics." *Earthquake Engineering & Structural Dynamics*, John Wiley & Sons, Ltd, 5(3), 283–292.

Lagomarsino, S., and Resemini, S. (2009). "The Assessment of Damage Limitation State in the Seismic Analysis of Monumental Buildings." *dx.doi.org*, 25(2), 323–346.

Lourenço, P. B. (2002). "Computations on historic masonry structures." *Progress in Structural Engineering and Materials*, John Wiley & Sons, Ltd., 4(3), 301–319.

Lourenço, P. B., Krakowiak, K. J., Fernandes, F. M., and Ramos, L. F. (2007). "Failure analysis of Monastery of Jerónimos, Lisbon: How to learn from sophisticated numerical models." *Engineering Failure Analysis*, 14(2), 280–300.

Lourenço, P. B., Mendes, N., Ramos, L. F., and Oliveira, D. V. (2011). "Analysis of Masonry Structures Without Box Behavior." *International Journal of Architectural Heritage*, Taylor & Francis Group, 5(4-5), 369–382.

Maio, R., and Tsionis, G. (2016). "Seismic fragility curves for the European building stock: review and evaluation of existing fragility curves - EU Science Hub - European Commission." JRC Technical Report.

Masciotta, M.-G., Roque, J., Ramos, L. F., and Lourenço, P. B. (2016). "A multidisciplinary approach to assess the health state of heritage structures: The case study of the Church of Monastery of Jerónimos in Lisbon." *Construction and Building Materials*, 116, 169–187.

Milani, G. (2013). "Lesson learned after the Emilia-Romagna, Italy, 20–29 May 2012 earthquakes: A limit analysis insight on three masonry churches." *Engineering Failure Analysis*, 34, 761–778.

Milani, G., and Valente, M. (2015a). "Comparative pushover and limit analyses on seven masonry

churches damaged by the 2012 Emilia-Romagna (Italy) seismic events: Possibilities of non-linear finite elements compared with pre-assigned failure mechanisms." *Engineering Failure Analysis*, 47, 129–161.

Milani, G., and Valente, M. (2015b). "Failure analysis of seven masonry churches severely damaged during the 2012 Emilia-Romagna (Italy) earthquake: Non-linear dynamic analyses vs conventional static approaches." *Engineering Failure Analysis*, 54, 13–56.

Milani, G., and Venturini, G. (2011). "Automatic fragility curve evaluation of masonry churches accounting for partial collapses by means of 3D FE homogenized limit analysis." *Computers & Structures*, 89(17-18), 1628–1648.

Milani, G., and Venturini, G. (2013). "Safety Assessment of Four Masonry Churches by a Plate and Shell FE Nonlinear Approach." *Journal of Performance of Constructed Facilities*, 27(1), 27–42.

Peña, F., Lourenço, P. B., Mendes, N., and Oliveira, D. V. (2010). "Numerical models for the seismic assessment of an old masonry tower." *Engineering Structures*, 32(5), 1466–1478.

Ramos, L. F., Marques, L., Lourenço, P. B., De Roeck, G., Campos Costa, A., and Roque, J. (2010). "Monitoring historical masonry structures with operational modal analysis: Two case studies." *Mechanical Systems and Signal Processing*, 24(5), 1291–1305.

Roque, J. (2010). "Metodologia integrada para avaliação e mitigação da vulnerabilidade sísmica das construções históricas em alvenaria: A Igreja dos Jerónimos como caso de estudo." (Ph.D. thesis), University of Minho, Guimarães, Portugal.

Scotta, R., Vitaliani, R., Saetta, A., Oñate, E., and Hanganu, A. (2001). "A scalar damage model with a shear retention factor for the analysis of reinforced concrete structures: theory and validation." *Computers & Structures*, 79(7), 737–755.

Sousa, M. L. (2006). "Risco sísmico em Portugal Continental."

TNO Building and Construction. (2016). "DIANA FEA: Release 10.1." TNO DIANA, The Netherlands.

Valente, M., and Milani, G. (2016). “Seismic assessment of historical masonry towers by means of simplified approaches and standard FEM.” *Construction and Building Materials*, 108, 74–104.

This paper can be found at https://doi.org/10.1061/(ASCE)ST.1943-541X.0002437

Table 1: Correlation between numerical and experimental frequencies found for nave and columns

Numerical Mode Shapes		**Experimental Mode Shapes**		**Error (%)**
mode [#]	**frequency [Hz]**	**mode [#]**	**frequency [Hz]**	
Nave (global modes)				
1st	3.79	1st	3.69	2.6
4th	5.34	2nd	5.12	4.1
7th	6.23	3rd	6.29	1.0
10th	6.61	4th	7.23	9.4
Columns of the nave (local modes)				
15th	7.39	1rd	7.36	0,4
16th	7,51	2th	7.52	0,1

Table 2: Seismic scenarios adopted and main parameters of the corresponding artificial records

Return Period	Magnitude	PGA [g]	Frequency Domain [Hz]	Duration [s]	Input ID
475 years	M_w=7.4	0.10	5.60	10.20	475_M74_1
		0.09	5.60	10.60	475_M74_2
		0.12	3.00	7.70	475_M74_3
975 years	M_w=7.8	0.17	4.50	14.90	975_M78_1
		0.16	7.10	13.90	975_M78_2
		0.14	5.60	15.00	975_M78_3
5000 years	M_w=8.2	0.21	3.00	20.29	5000_M82_1
		0.23	5.60	20.71	5000_M82_2
		0.21	3.60	20.75	5000_M82_3

This paper can be found at https://doi.org/10.1061/(ASCE)ST.1943-541X.0002437

Figure 1: Monastery of Jerónimos: (a) external view of the complex; and (b) outer view of the church

This paper can be found at https://doi.org/10.1061/(ASCE)ST.1943-541X.0002437

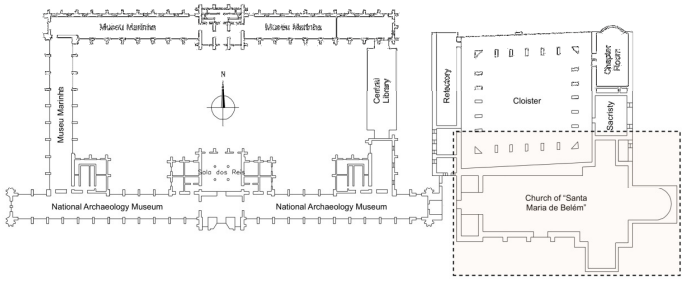

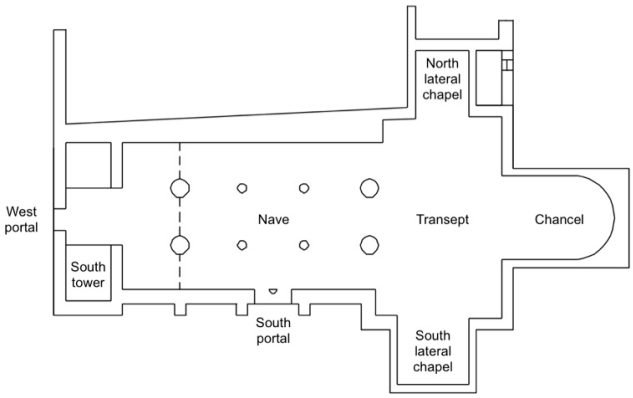

Figure 2: Monastery of Jerónimos complex: (a) plan of the two courts; (b) plan of Santa Maria de Belém church; (c) view to the ribbed vault.

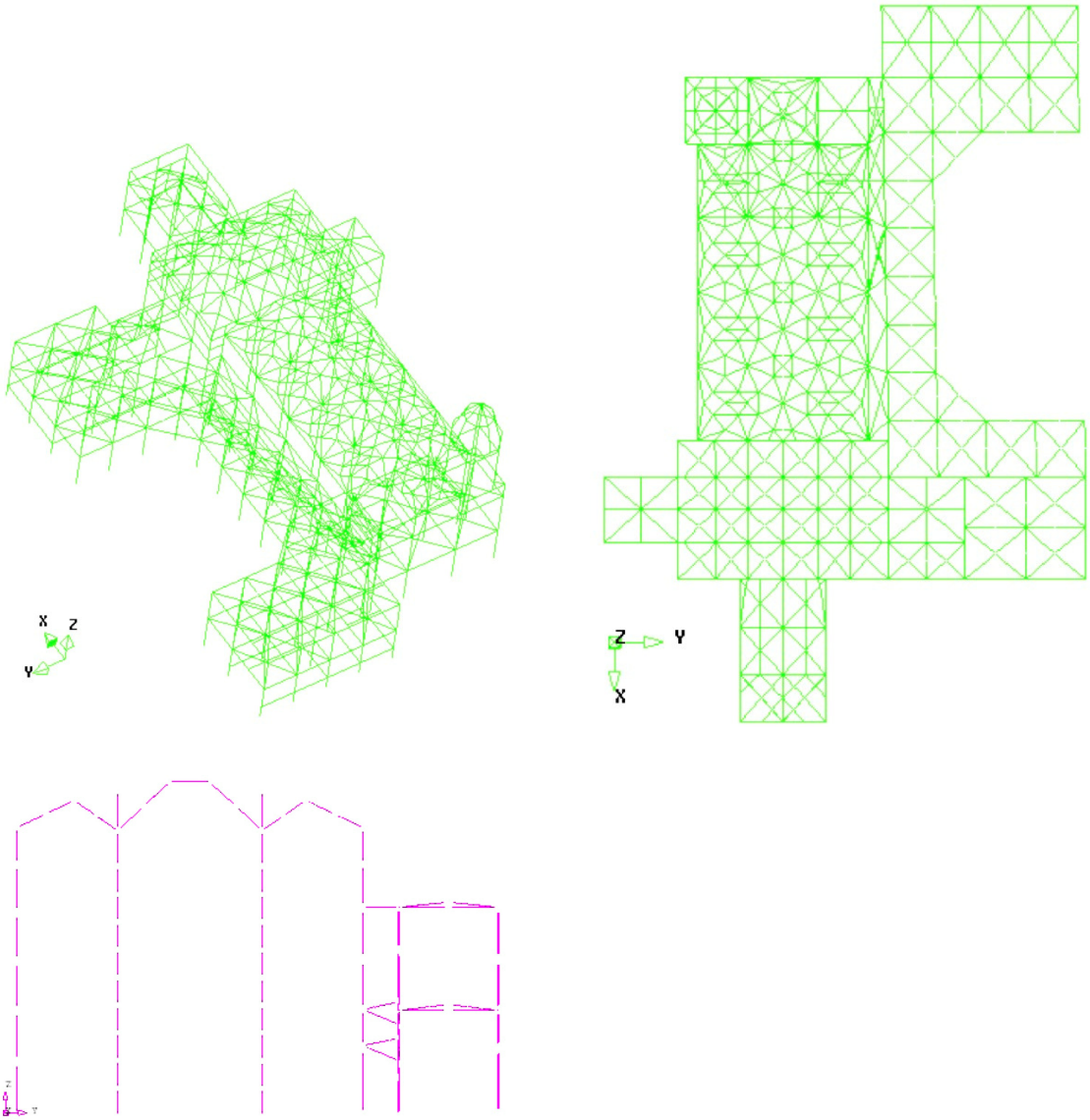

Figure 3: Finite element model: (a) 3D view; (b) plan view; (c) central arcade of the nave in transversal direction, adapted from (Masciotta et al. 2016).

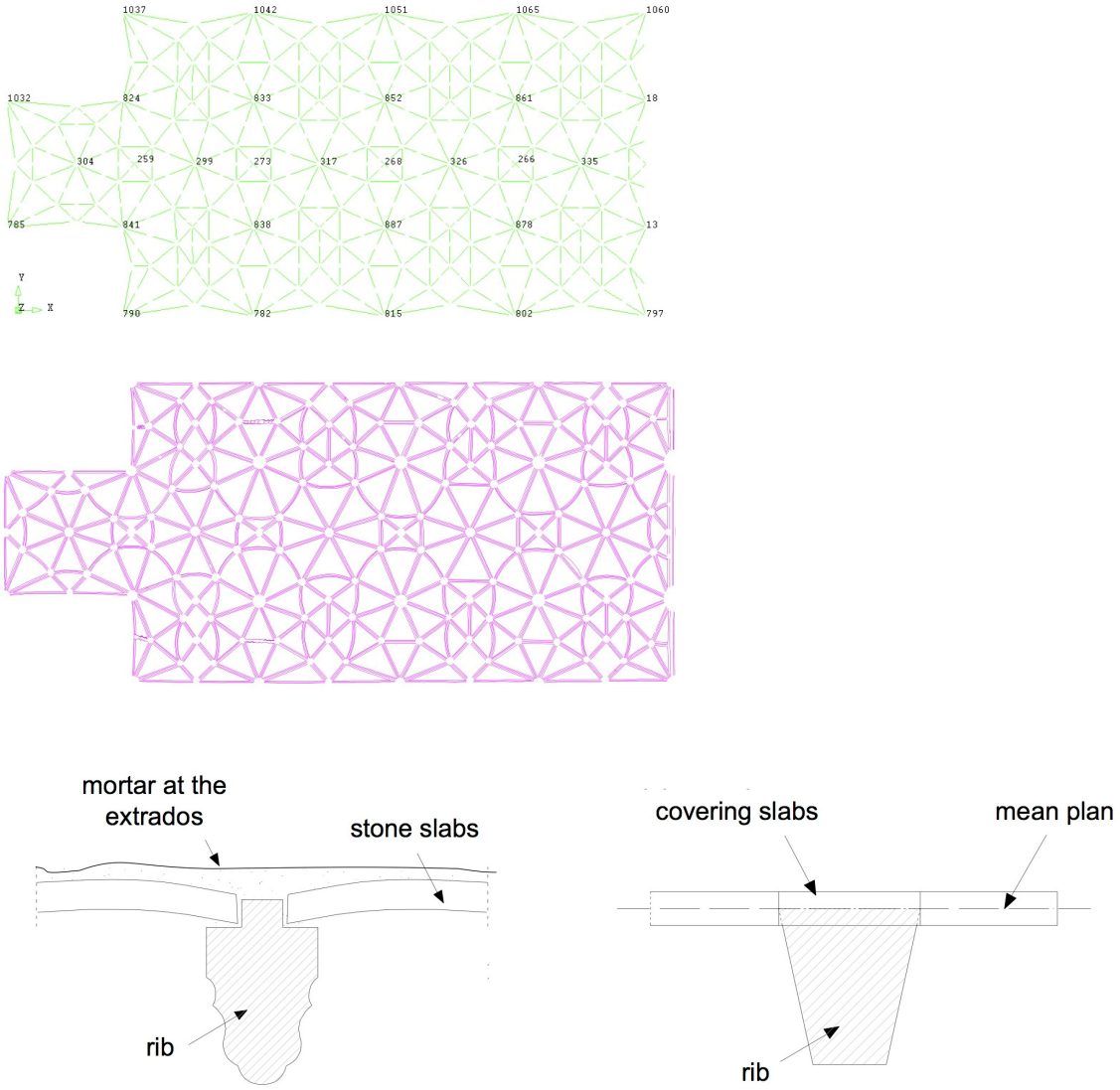

Figure 4: Finite element model: (a) actual and (b) approximated configuration of the nave vaults; (c) existing and (d) geometric model adopted for the rib profiles of the vaults.

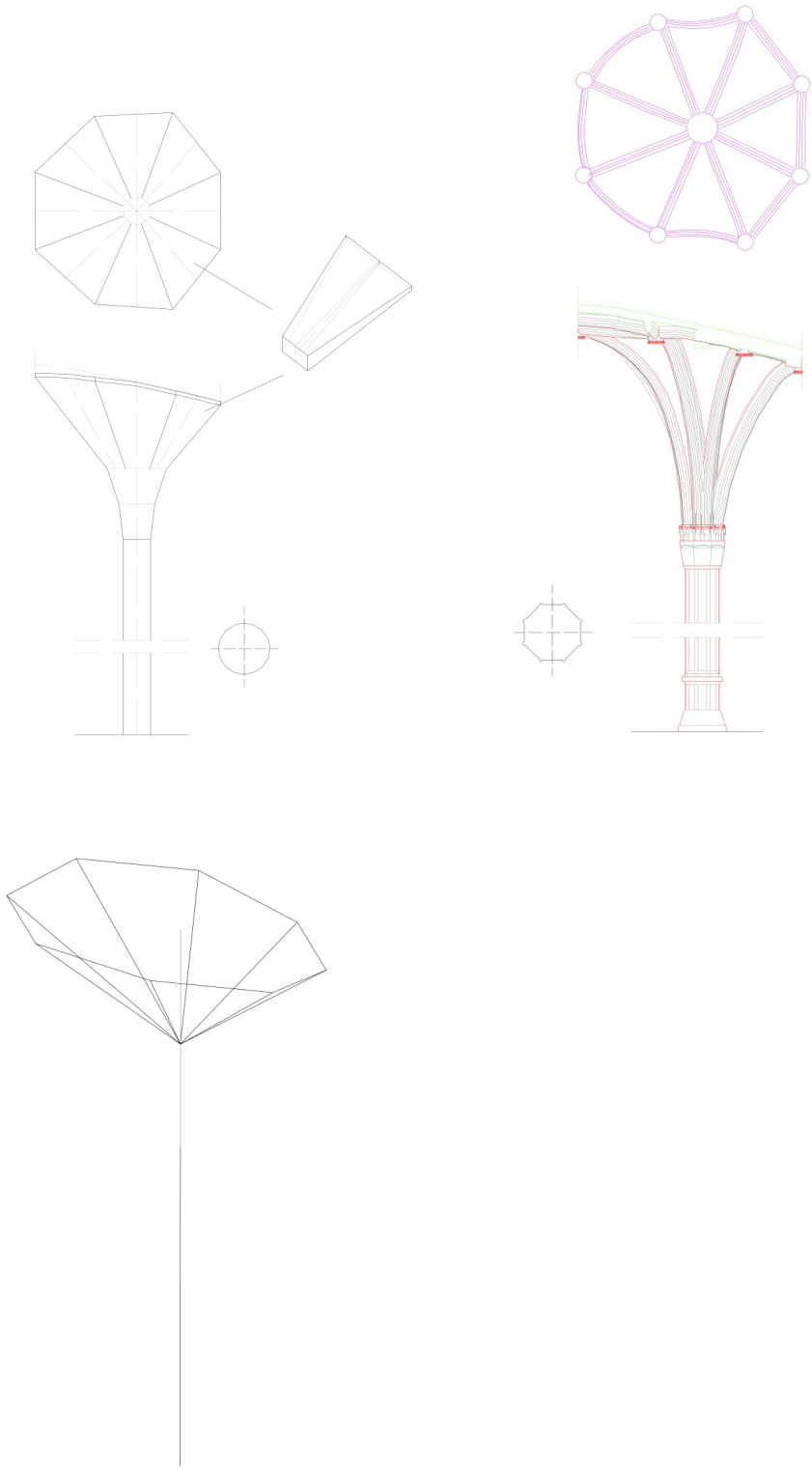

Figure 5: Finite element model: (a) existing; (b) approximated configuration; (c) geometric model adopted for the columns, adapted from (Masciotta et al. 2016).

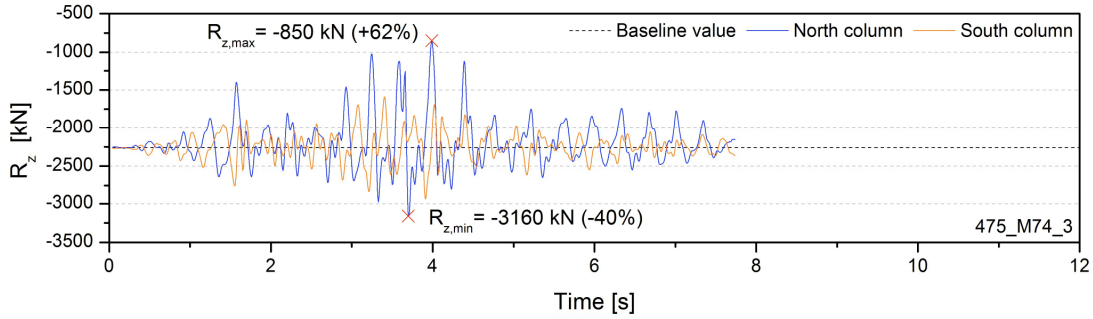

Figure 6: Time history of vertical reactions at the north and south columns for a return period of 475 years, (seismic input 475_M74_3)

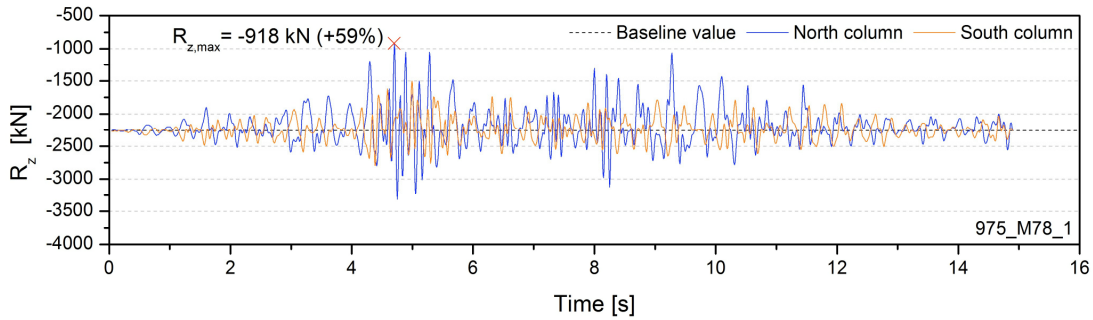

Figure 7: Time history of vertical reactions at the north and south columns for a return period of 975 years (seismic input 975_M78_1)

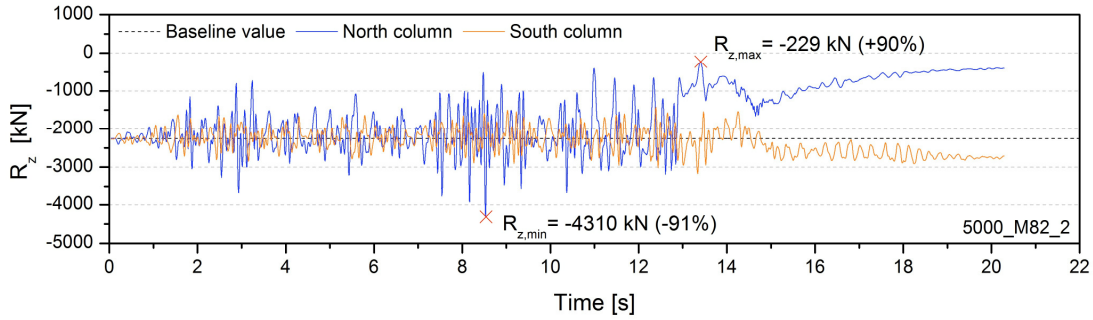

Figure 8: Time history of vertical reactions at the north and south column for a return period of 5000 years (seismic input 5000_M82_2)

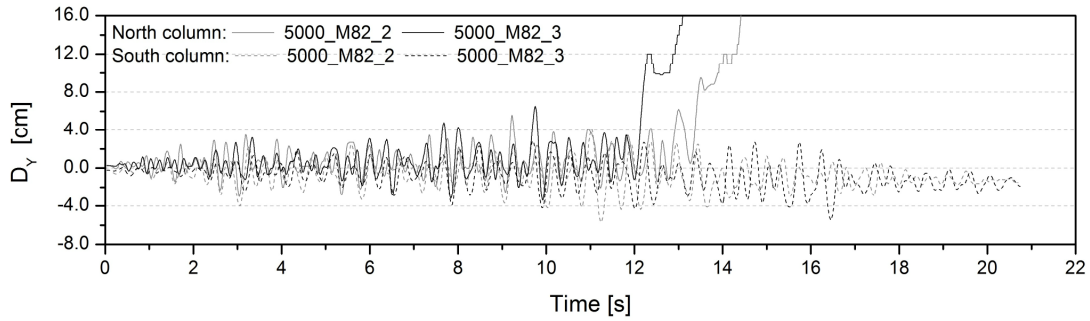

Figure 9: Time history of horizontal displacements at the shaft of the north and south columns.

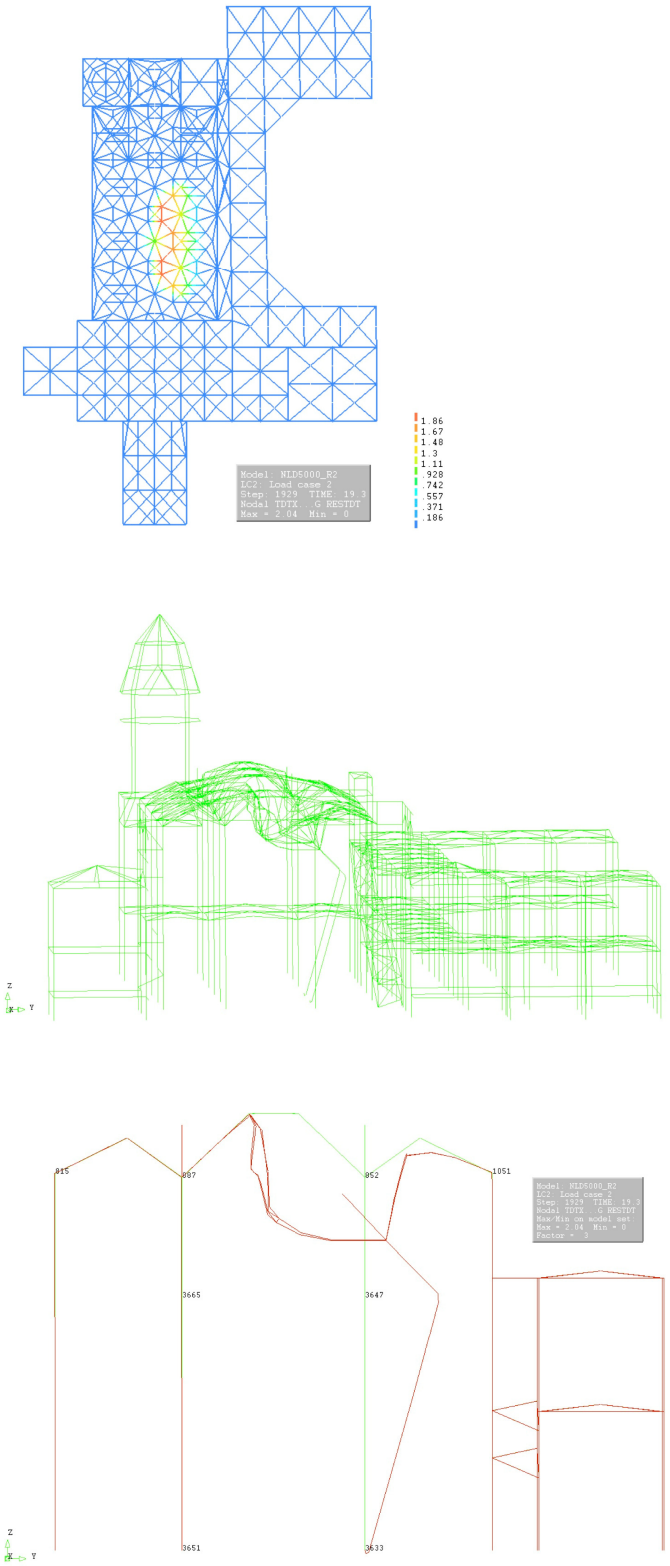

Figure 10: Configuration of the potential collapse mode for the analysis 5000_M82_2: (a) plan view; (b) perspective; (c) central arcade transversal to the nave.

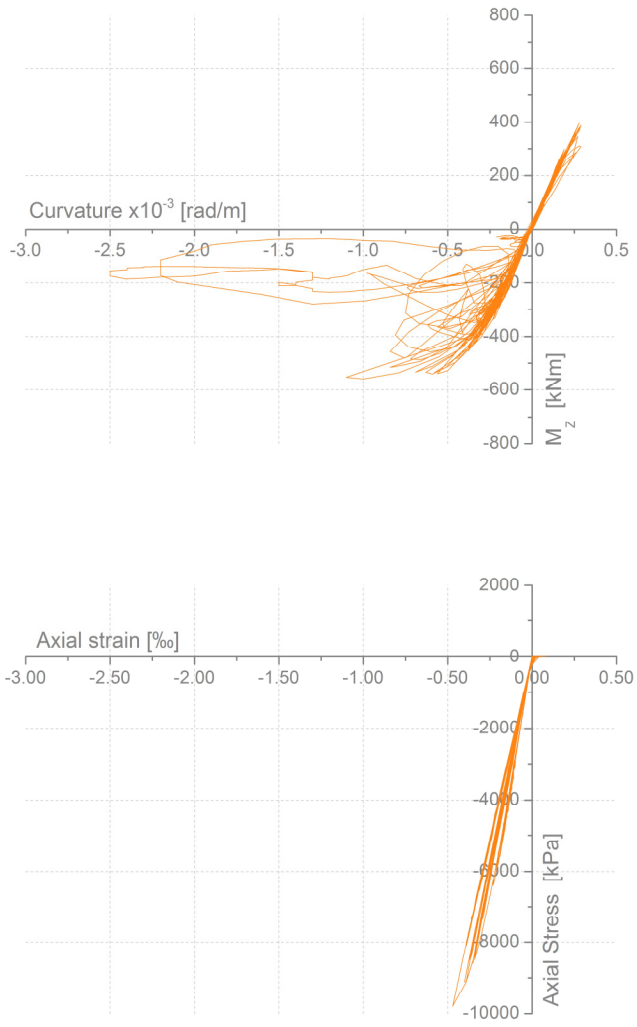

Figure 11: Response of the north column obtained from seismic input 5000_M82_2: (a) moment-curvature diagrams; (b) stress-strain curves of the most compressed fibres.

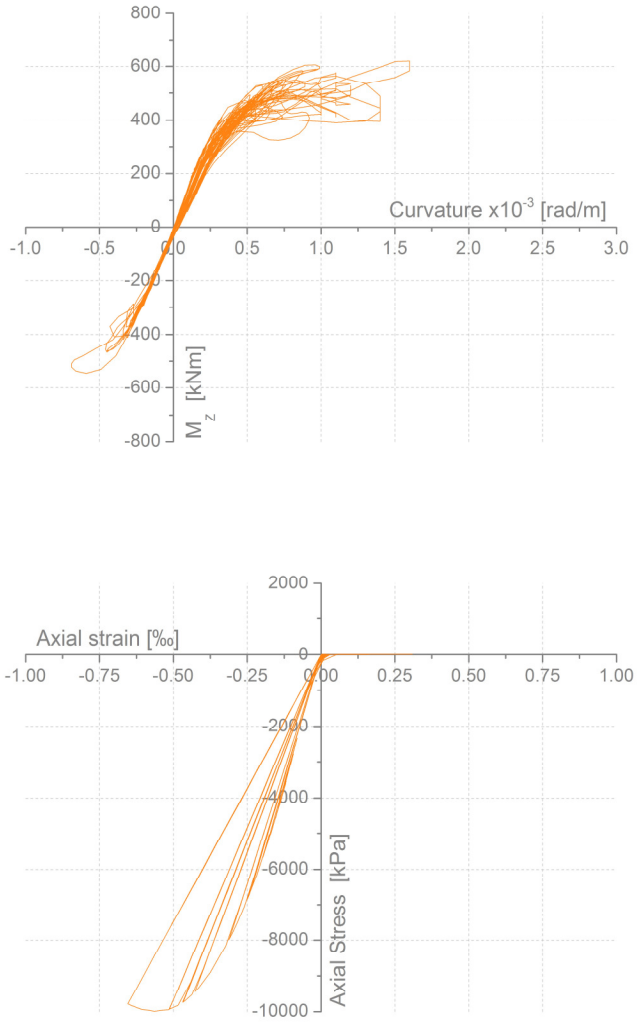

Figure 12: Response of the south column obtained from seismic input 5000_M82_2:

(a) moment-curvature diagrams; (b) stress-strain curves of the most compressed fibres.

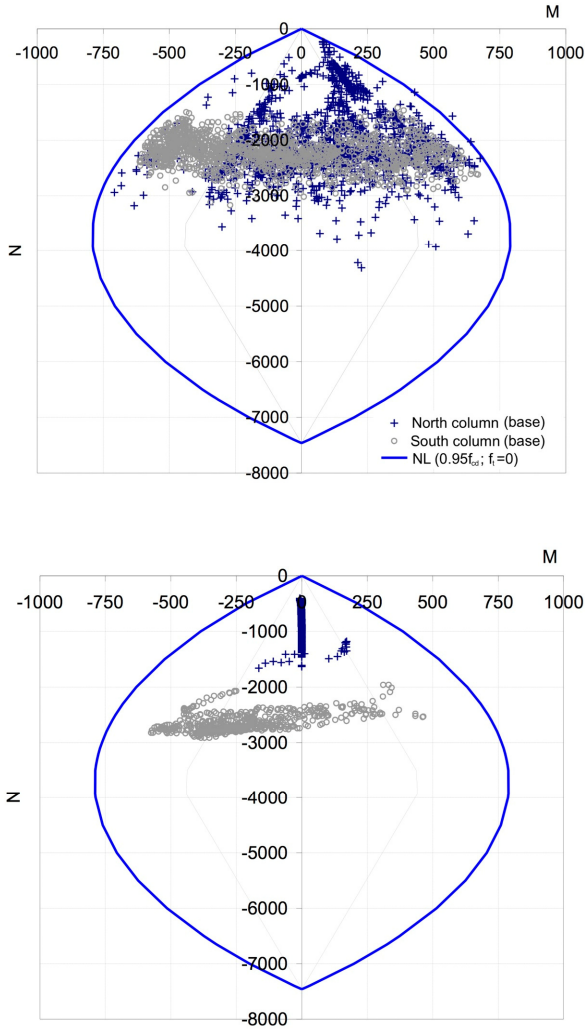

Figure 13: N-M interaction diagram at the base of the north and south columns: (a) before and (b) after the beginning of collapse (seismic input 5000_M82_2).

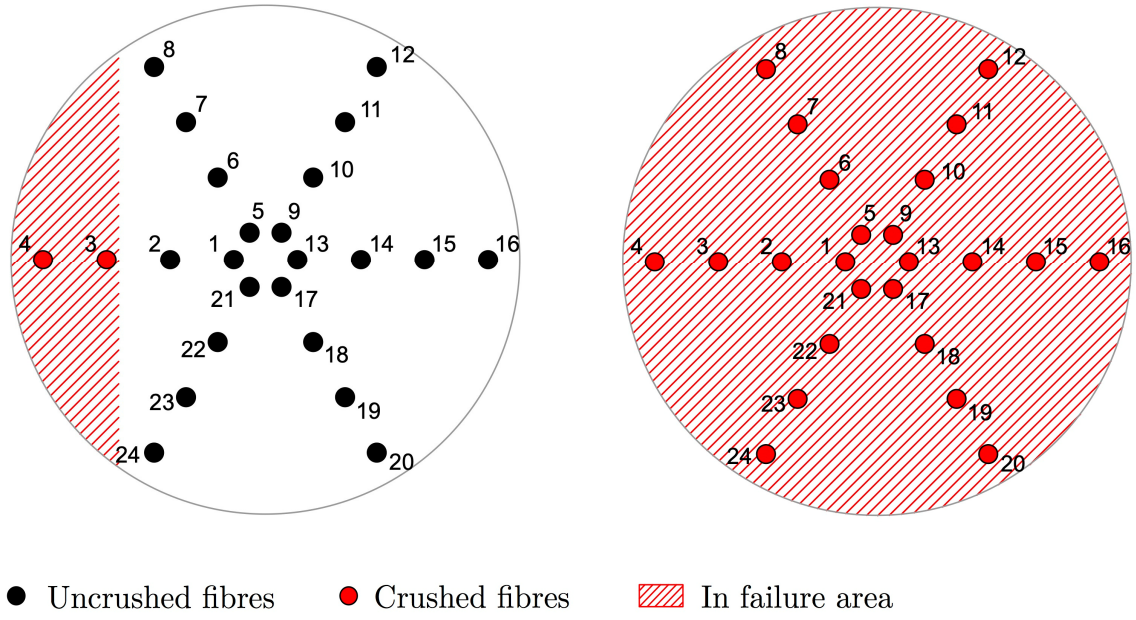

Figure 14: Schematic representation of the compressive damage in the middle section of the shaft and in bottom section of the north column (seismic input 5000_M82_2).

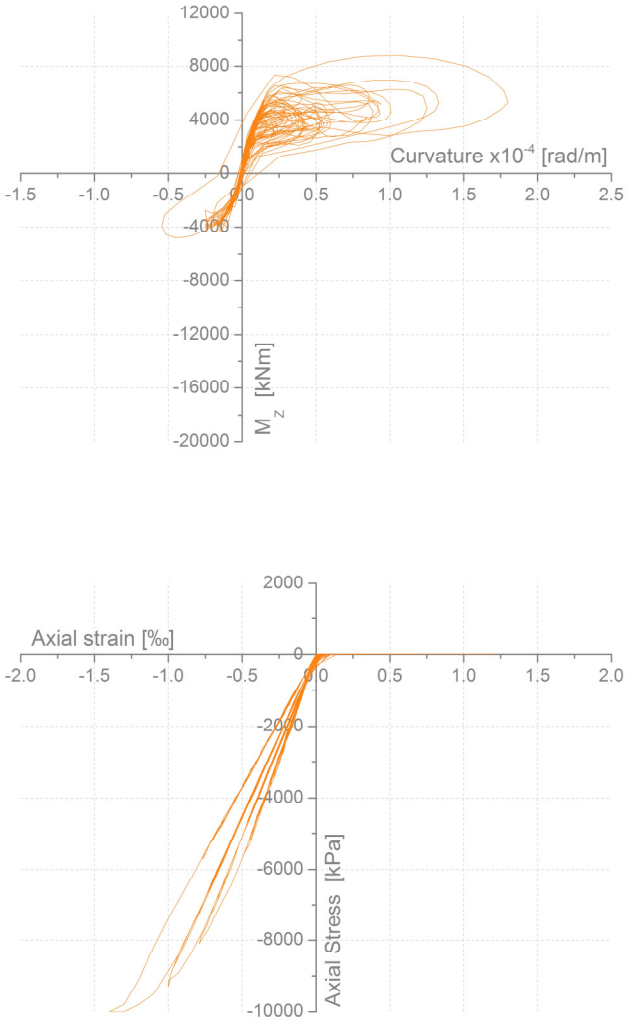

Figure 15: Response of the lateral walls, north and south, obtained with seismic input 5000_M82_2: (a) moment-curvature diagrams; (b) stress-strain curves for the most compressed fibres.

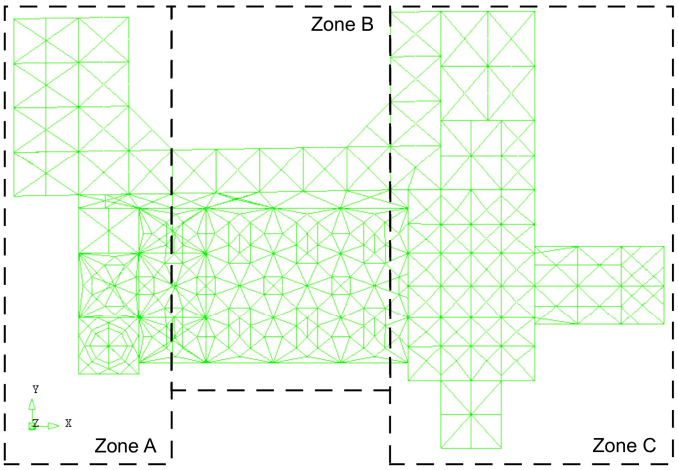

Figure 16: Plan view of the finite element model with the indication of sub-structures A, B and C.

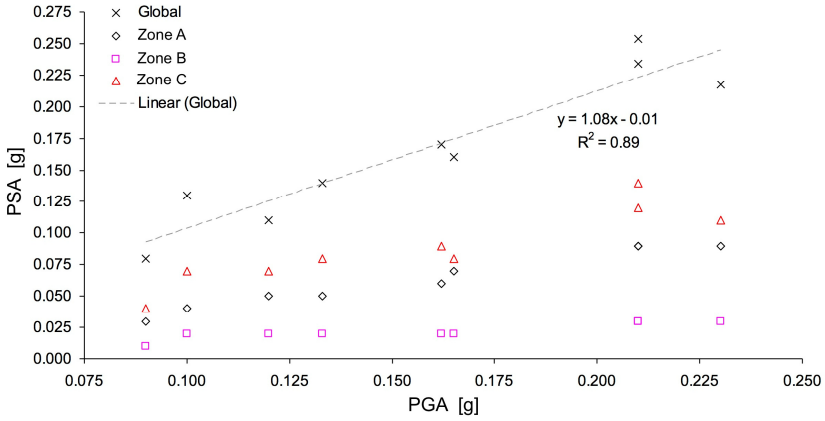

Figure 17: Base shear coefficients (PSA) versus peak ground acceleration (PGA) of the seismic inputs used (average maximum values per structural zone A, B and C).

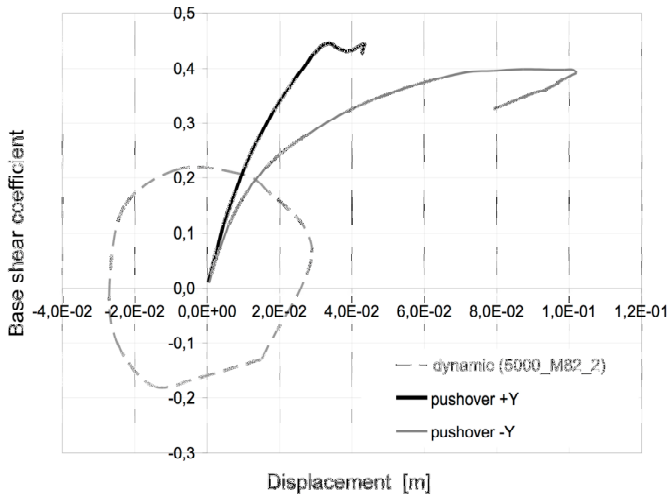

Figure 18: Envelope of the dynamic base shear versus uniform pushover capacity curves (+Y, -Y).

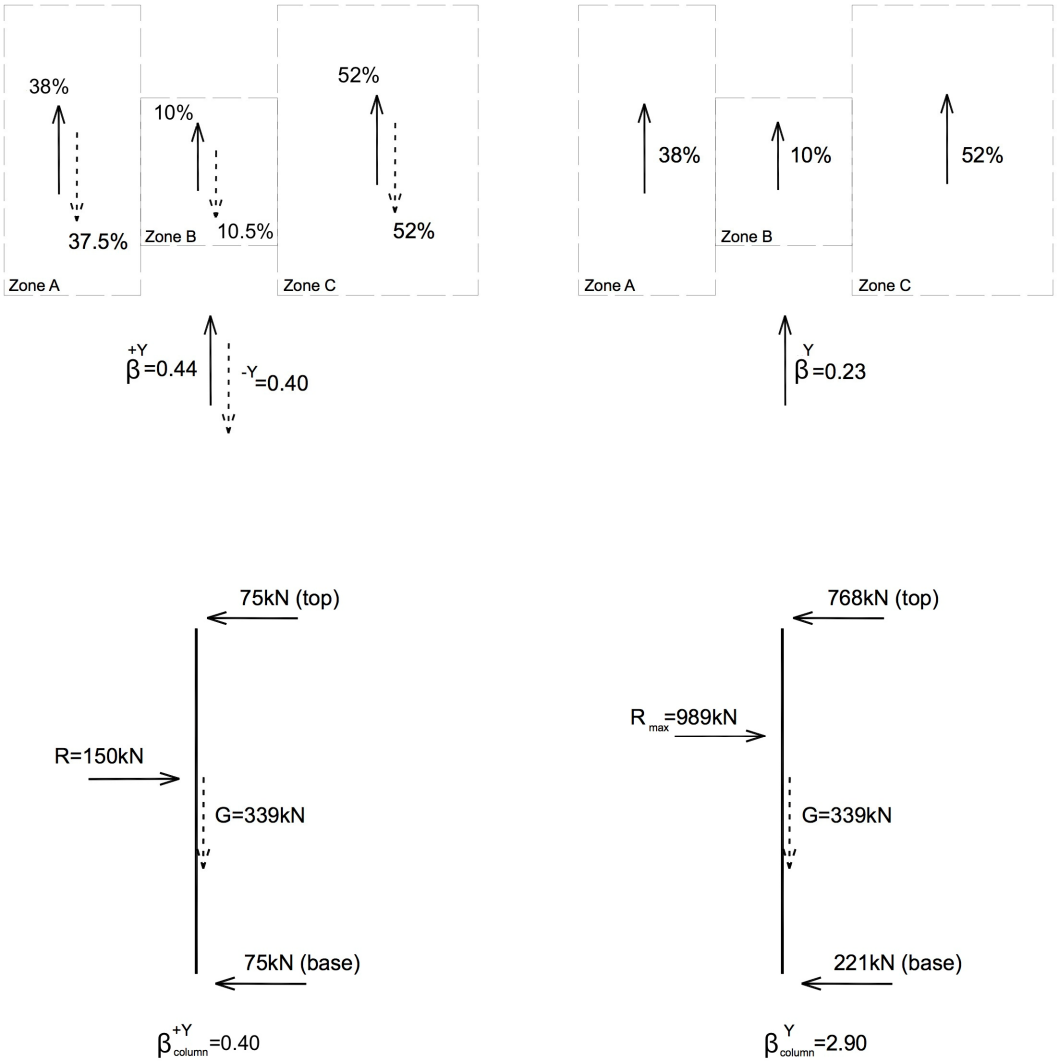

Figure 19: Static base shear (uniform pushover, +Y and –Y) versus envelope of dynamic base shear (seismic input 5000_M82_2): (a) percentage of in-plan distribution; and (b) central north column of the nave (zone B).

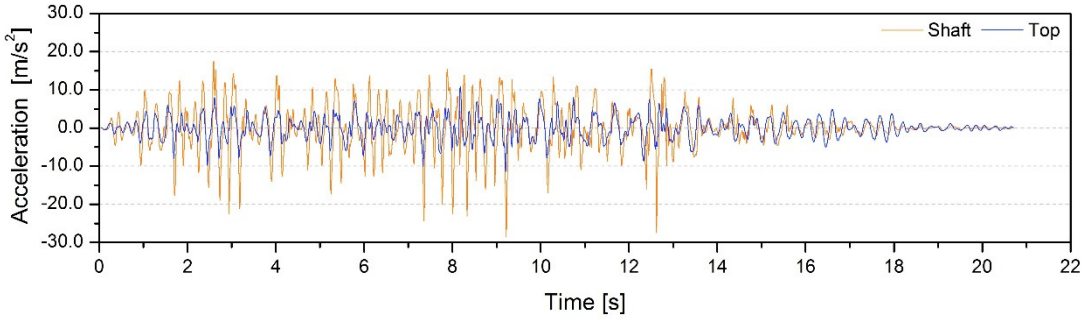

Figure 20: Time history of accelerations in the north column shaft (at the top and middle section) for seismic input 5000_M82_2.

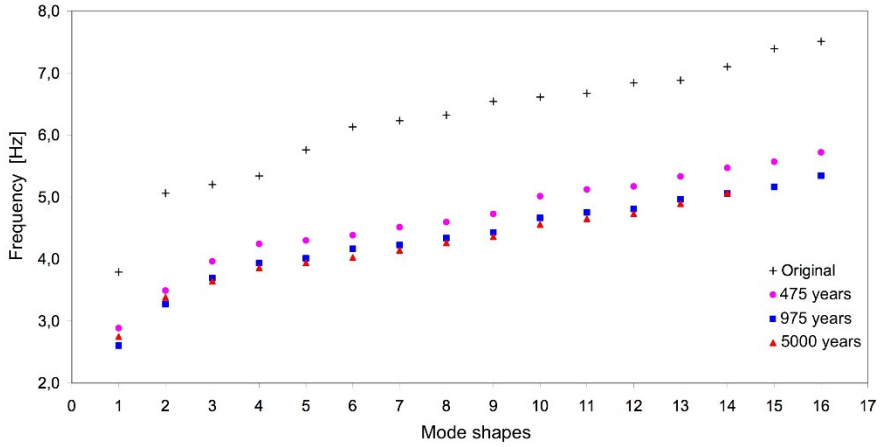

Figure 21: Modal frequencies of the church, before and after seismic excitations (average values per return period).